

# HUMPS IN DARK I-V-CURVES – ANALYSIS AND EXPLANATION

Jutta Beier, Bernhard Voß  
 Fraunhofer-Institut für Solare Energiesysteme (ISE)  
 Oltmannsstr. 22  
 W-7800 Freiburg  
 Germany  
 Tel. +49 (761) 4014-142  
 Fax +49 (761) 4014-100

## ABSTRACT

Analysing a large number of dark and light I-V-curves of different kinds of solar cells [1], we noticed two main discrepancies between the measured curves and the two-diode model which was used for the analysis:

- the value of the diode quality factor of the recombination current,  $n_2$ , more often than not differs from the usually assumed value of  $n_2=2$
- some I-V-curves show an additional structure ("hump") in the voltage range corresponding to the recombination current which can not be described by varying the value of  $n_2$ .

In this work we give a quantitative analysis and explanation for the observed humps. Starting from their mathematical description, the other forms of deviation from the usual two-diode model are derived.

## INTRODUCTION

Dark I-V-curves of solar cells are an important means of characterising the cells. Besides the diagnostic value of the dark I-V-curves, they allow - under certain conditions - to predict the efficiencies of the solar cells under different illumination levels via the superposition principle.

Within the scope of investigations concerning the superposition principle, a large data base of dark and light I-V-curves of many different solar cells (commercially available Si cells, high efficiency Si cells and GaAs-cells prepared at ISE) at different illumination levels and temperatures has been collected.

The analysis of the I-V-curves using the two-diode model with the series resistance  $R_s$ , shunt resistance  $R_p$ , recombination current of the space charge layer  $\{J_{02}, n_2\}$  and the Shockley diode current  $J_{01}$  of the cell,

$$J = J_{01}(\exp(q(V-R_s J)/kT) - 1) + J_{02}(\exp(q(V-R_s J)/n_2 kT) - 1) + (V-R_s J)/R_p \quad (1)$$

showed that for the commercial Si cells, the value of  $n_2$  deviates from the theoretically assumed value  $n_2=2$ . The form of these deviations was such that by choosing  $n_2 \neq 2$  the I-V-curves were fitted very well.

However, the I-V-curves of the high efficiency cells showed an additional structure ("hump") in the lower voltage range (approx. 0.1 .. 0.5 V) corresponding to the recombination current, which could not be described at all by varying the value of the diode quality factor  $n_2$  [1].

Although  $n_2=2$  is often stated to be the "only physically meaningful value", a discrepancy between this  $n_2=2$ -theory and experiment is to be expected:

It is only the very specific assumptions about the energy levels (middle of the bandgap,  $E_r = E_i$ ) and capture cross sections (equal for electrons and holes,  $c_p = c_n$ ) of the recombination centres in a symmetrically doped diode which lead to the usual two-diode model with  $n_2=2$ .

## APPROACH

In order to explain the observed "humps" and  $n_2 \neq 2$ -values, we determined the recombination current going back to the classical Sah-Noyce-Shockley-theory [2], where the recombination current is calculated as the integral of the recombination rate over the space charge region (SCR).

The result for the recombination current of Sah et al. is given in eq. 27 of [2]. Their integration limits implicitly assume a symmetrically doped diode ( $n_n = p_p$ , where  $n(p)_{n(p)}$  = concentration of electrons (holes) on the n(p)-doped side). In order to discuss their results, they then extend the integration limits to 0 and  $\infty$ . In [3] it is shown that the extension of the integration limits in fact is valid only for symmetrical junctions, when additionally the recombination lifetimes for electrons and holes are equal,  $\tau_{n0} = \tau_{p0}$ . As solar cells are always asymmetrically doped, these special results are not applicable here.

But the integral can be solved analytically, so that the restrictions concerning the parameters are not necessary. The result for the recombination current is then

$$J_{rg} = \frac{2 q n_i \cdot \sinh[qV/2kT]}{(\tau_{p0}\tau_{n0})^{1/2}} \cdot \frac{W}{\theta} \cdot f(b), \quad (2)$$

with

$$W = \text{width of the space charge region} \quad (3)$$

$$\theta = q(\psi_d - V)/kT, \quad \psi_d = \text{built-in voltage} \quad (4)$$

$$f(b) = (1-b^2)^{-1/2} \cdot \arctan[\alpha/\beta \cdot (1-b^2)^{1/2}] \quad \text{for } b^2 < 1 \quad (5)$$

$$f(b) = (b^2-1)^{-1/2} \cdot \operatorname{arctanh}[\alpha/\beta \cdot (b^2-1)^{1/2}] \quad \text{for } b^2 > 1 \quad (6)$$

$$f(b) = \alpha/\beta \quad \text{for } b^2 = 1, \quad (7)$$

where

$$b = \exp[-q/(2kT)] \cdot \cosh[(E_r - E_{r0})/kT] \quad (8)$$

$$E_{r0} = E_i - 1/2 \cdot kT \cdot \ln(\tau_{p0}/\tau_{n0}) \quad (9)$$

$$\alpha = 2 \sinh(\theta/2) \quad (10)$$

$$\beta = (\tau_{n0} \cdot p_p / \tau_{p0} \cdot n_n)^{1/2} + (\tau_{p0} \cdot n_n / \tau_{n0} \cdot p_p)^{1/2} + 2b \cdot \cosh(\theta/2) \quad (11)$$

$$\tau_{n,p0} = 1/(N_r c_{n,p}), \quad N_r = \text{concentration of rec. centres} \\ c_{n,p} = \text{capture cross section for electrons or holes} \quad (12)$$

In summary,  $J_{rg}$  is the current which originates from recombination via a recombination centre in the SCR with an energy level  $E_r$  and the recombination parameters  $\tau_{p0}$  and  $\tau_{n0}$ .

The factor  $\sinh(qV/2kT)$  corresponds to the usual two-diode model with  $n_2 = 2$ . Thus, the factors

- $W/\theta$  and
- $f(b)$

have to be responsible for the deviations from the two-diode model observed in measurements. The voltage dependence of these quantities and the influence of the recombination parameters  $\tau_{p0}$ ,  $\tau_{n0}$  and  $E_r$  on  $f(b)$  and by that on the I-V-curves will be discussed in the following sections.

#### The factor $W/\theta$

For voltages up to about 0.5V, the width  $W$  of the SCR is calculated as a function of the capacitance of the SCR  $C = C(V)$  using the model for  $C(V)$  developed by Chawla and Gummel [4]. For voltages of about 0.6V or higher, the results of Liou and Lindholm [5] for  $W(V)$  are used. In the intermediate region, the  $W$ -data thus gained are interpolated.

The  $W(V)$ -values of the lower voltage regime are calculated by an implicit equation. Therefore, the slope of

the  $W(V)$ -curve is unknown, and a small change of the slope at the transition to the interpolated curve occurs.

The built-in voltage  $\psi_d$  is calculated following Chawla and Gummel. They show, that the usual expressions for  $\psi_d$  in the case of the linearly graded or abrupt junction have to be replaced by the so called gradient voltage  $V_g$ , which takes into account the free charge carriers in the SCR.

Fig.1 shows the voltage dependence of the factor  $W/\theta$  calculated in accordance with [4], compared with the values resulting from the assumption of a linearly graded or an abrupt junction. For the calculations, the value for the doping concentration gradient at the junction is needed. It is determined from the base doping  $N_B$ , doping concentration at the surface of the emitter  $C_s$ , thickness of the emitter  $d$  and doping profile (Gauss or erfc), taking into account the constance of the phosphorus concentration at the emitter surface [6]. In the example shown, these quantities are  $N_B = 1.5 \cdot 10^{16} \text{ cm}^{-3}$ ,  $C_s = 2 \cdot 10^{19} \text{ cm}^{-3}$ ,  $d = 0.6 \mu\text{m}$  =  $a = 3.6 \cdot 10^{21} \text{ cm}^{-4}$ .

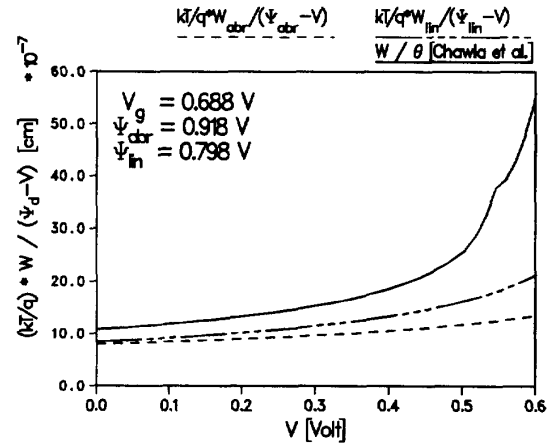


Fig.1: Values of the expression  $W/\theta = W/(V - V_g)$ . For comparison, the analogous expressions for linearly graded and abrupt junctions are also shown [1].

Although the voltage dependencies of the three curves differ from each other, their difference is too small to account for the observed deviations from the two-diode model.

#### The factor $f(b)$

The voltage dependence of  $f(b(V))$  is given by eqs.(5)-(11).

In fig.2,  $f(b)$  is shown for a varying ratio  $\tau_{n0}/\tau_{p0}$ , with the same cell doping parameters as in fig.1. As an example,  $E_r - E_{r0} = \pm 8kT$  was chosen.

voltage regime	f(b)	J <sub>rg</sub>
small forward voltages, $b \gg 1$ , $\theta/2 \gg 1$	about $\sim \exp(qV/2kT)$	about $\sim \exp(qV/kT)$
voltages about $V(\max)$ , see eq....	maximum	$\sim \exp(qV/2kT)$
higher forward voltages, $b < 1$ , but $\theta/2 > 1$ : a) $(\tau_{n0} \cdot p_p / \tau_{p0} \cdot n_n)^{\pm 1/2} \gg 1$ b) $(\tau_{n0} \cdot p_p / \tau_{p0} \cdot n_n)^{\pm 1/2} \approx 1$	a) $\sim \exp(-qV/2kT)$ b) constant	a) saturation of J <sub>rg</sub> b) $\sim \exp(qV/2kT)$

Tab.1: Voltage dependence of f(b) and J<sub>rg</sub> in different voltage regimes

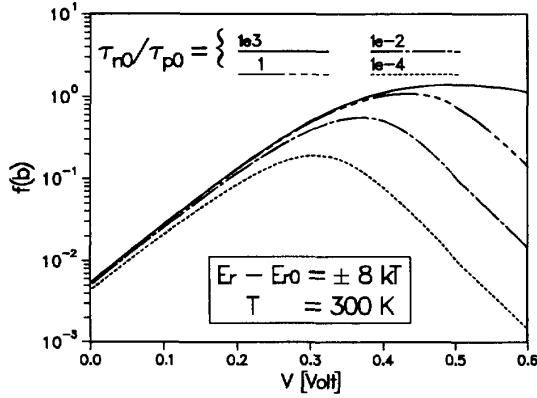


Fig.2: f(b(V)) for different values of  $\tau_{n0}/\tau_{p0}$ . As an example,  $(E_r - E_{r0}) = \pm 8kT$  was chosen. [1]

$(E_r - E_{r0})$  is a measure of the energetic distance of the recombination centre to the intrinsic energy level  $E_i$  (see eq.8 and 9).

By analysing eq.(5)-(11), the voltage where the maximum of f(b) occurs is calculated to be

$$V(\max) = \frac{V_g}{2} + \frac{kT}{q} \cdot \ln(\cosh[(E_r - E_{r0})/kT]) - \frac{kT}{q} \cdot \ln((\tau_{n0} \cdot p_p / \tau_{p0} \cdot n_n)^{1/2} + (\tau_{p0} \cdot n_n / \tau_{n0} \cdot p_p)^{1/2}) \quad (13)$$

which is in agreement with the curves in fig.2. Together with the factor  $\sinh(qV/2kT)$  in eq.2, there follows an exponential voltage dependence for J<sub>rg</sub> in the form of  $\exp(qV/2kT)$  in this voltage regime.

At smaller voltages, f(b) varies roughly as  $\exp(qV/2kT)$  and is independent of  $\tau_{n0}/\tau_{p0}$ , which again agrees with the curves in fig.2. The resulting voltage dependence for J<sub>rg</sub> is  $\exp(qV/kT)$  here.

The shape of the curve f(b) at voltages higher than  $V(\max)$  depends on the value of  $\tau_{n0} \cdot p_p / \tau_{p0} \cdot n_n$ . If either

$$(\tau_{n0} \cdot p_p / \tau_{p0} \cdot n_n)^{1/2} \gg 1 \text{ or } (\tau_{p0} \cdot n_n / \tau_{n0} \cdot p_p)^{1/2} \gg 1$$

applies (for Si solar cells e.g. the second condition), an exponential decrease of f(b) is obtained,

$$f(b(V)) \approx (\tau_{n0} \cdot p_p / \tau_{p0} \cdot n_n)^{1/2} \cdot e^{qV_g/2kT} \cdot e^{-qV/2kT} \quad (14)$$

Together with the  $\sinh(qV/2kT)$  from eq.2, a saturation of J<sub>rg</sub> at the value

$$J_{rg} \approx q \cdot \frac{n_i}{\tau_{p0}} \cdot \frac{W}{\theta} \cdot (p_p/n_n)^{1/2} \cdot e^{qV_g/2kT} \quad (15)$$

sets in.

But if  $\tau_{n0} \cdot p_p / \tau_{p0} \cdot n_n \approx 1$ , f(b) varies only weakly. This can be seen in fig.2 in those curves where  $\tau_{n0}/\tau_{p0} = 10^3$ , because for the underlying solar cell parameters, the ratio  $n_n/p_p$  is about  $n_n/p_p \approx 10^3$  and thus  $\tau_{n0} \cdot p_p / \tau_{p0} \cdot n_n \approx 1$  applies.

In this case, the voltage dependence of J<sub>rg</sub> is  $\exp(qV/2kT)$ .

The voltage dependences of f(b) and J<sub>rg</sub> are summarised in tab.1.

## RESULTING THEORETICAL CURVES

In this section, the total shape of the I-V-curves will be discussed, where the current contribution of the recombination current of the SCR is calculated according to the preceding paragraphs.

### Recombination parameter dependence of the I-V-curves

From the results of the above curve discussion, the origin of the deviations of I-V-curves from the usual two-diode model becomes clear:

In the case of a symmetrically doped diode ( $p_p = n_n$ ) discussed in [2], with the assumptions  $\tau_{n0} = \tau_{p0}$  and  $E_r = E_{r'}$ , i.e.  $E_r = E_{r0}$ , an almost constant f(b) results in the voltage regime relevant for the recombination current (up to about 0.5V). The voltage dependence  $\exp(qV/2kT)$  of the

recombination current following from this corresponds to the two-diode model of eq.1 with  $n_2 = 2$ .

The same is true for an asymmetrical junction with an acceptorlike recombination centre,  $\tau_{p0} < \tau_{n0}$ . It cancels the asymmetry of the pn-junction so that  $\tau_{n0} \cdot p_p / \tau_{p0} \cdot n_n \approx 1$ , and again the voltage dependence of eq.1 for  $J_{rg}$  results.

But if an asymmetrical junction with a donorlike recombination centre,  $\tau_{n0} < \tau_{p0}$ , is considered, which enhances the asymmetry,

$$\tau_{p0} \cdot n_n / \tau_{n0} \cdot p_p \gg 1$$

the exponential decrease of  $f(b)$  derived above and thus the saturation of the recombination current sets in. Together with the term  $J_{01} \cdot \exp(qV/kT)$ , which dominates for voltages about  $V \approx 0.5V$ , the picture of a "hump" in the total I-V-curve arises.

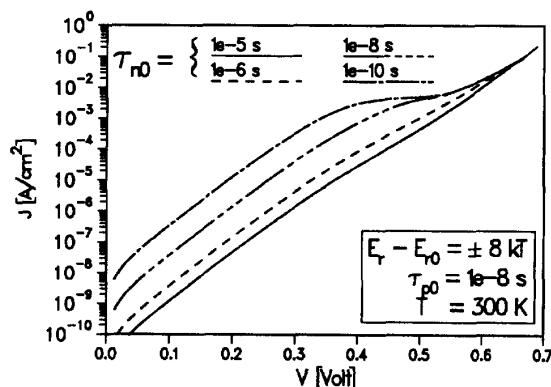


Fig.3: Dark I-V-curves with  $J_{01} = 6 \cdot 10^{-13} \text{ A/cm}^2$  for different values of  $\tau_{n0}/\tau_{p0}$ . As an example,  $(E_r - E_0) = \pm 8kT$  was chosen.  $R_p$  and  $R_s$  are ideal

This is shown in fig.3. The curves are calculated for the same cell parameters as for fig.1 and fig.2; as an example,  $(E_r - E_0) = \pm 8kT$  was chosen. The smaller  $\tau_{n0}$  and thus the larger  $\tau_{p0} \cdot n_n / \tau_{n0} \cdot p_p$  becomes, the clearer the hump arises.

#### Temperature dependence of the I-V-curves

For solar cells with  $\tau_{n0} \cdot p_p / \tau_{p0} \cdot n_n \approx 1$ , the resulting temperature dependence is that caused by the factors  $n_i/\theta \sim T^{5/2} \cdot \exp(-E_{gap}(T)/2kT)$ . This well-known form of T-dependence is shown in fig. 4a. The values of  $J_{01}$  needed for the calculations were determined using  $J_{01}(T) \sim n_i^2(T)$ , with  $J_{01}(300K) = 6 \cdot 10^{-13} \text{ A/cm}^2$  and  $n_i(T)$ -data taken from [7].

On the other hand, for cells where the recombination current saturates (hump) with increasing voltage, a saturation also with respect to the temperature occurs:

As eq.15 shows, the exponentially increasing factor  $n_i(T)$  is compensated by the term  $\exp(qV(T)/2kT)$ , from where an almost temperatureindependent  $J_{rg}$  in the regime of the voltage saturation and a very characteristic temperature dependence results (fig. 4b).

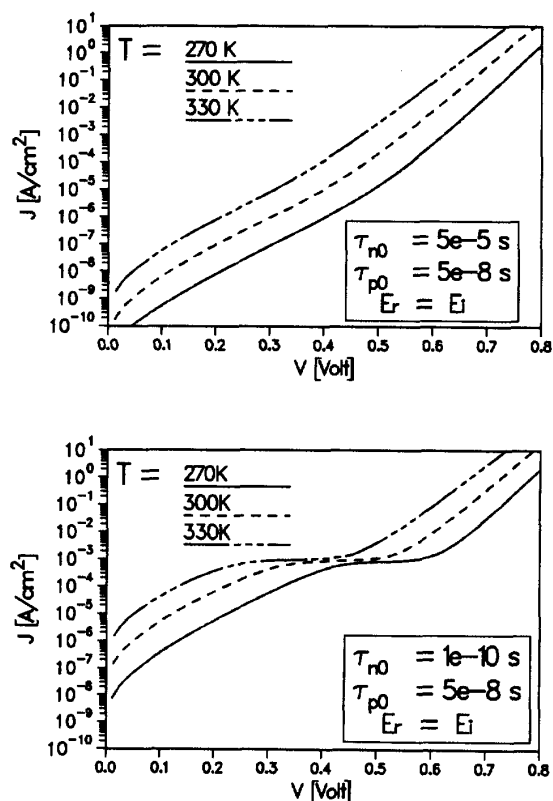


Fig.4: Temperature dependence of dark I-V-curves with  $J_{01}(300K) = 6 \cdot 10^{-13} \text{ A/cm}^2$  and

- $\tau_{p0} \cdot n_n / \tau_{n0} \cdot p_p \approx 1$
- $\tau_{p0} \cdot n_n / \tau_{n0} \cdot p_p \gg 1$

#### EXPERIMENTAL DATA AND RESULTS OF FITS

The characteristic structures in the I-V-curves derived above result from a single recombination centre. Many measured I-V-curves of high efficiency cells show these humps and especially the striking temperature dependence of the humps. Therefore, we tried to confirm the assumption that these measured humps are to be traced back to one

single recombination centre by fitting eq.2 to the forward I-V-curves.

Two examples of measured (symbols) and fitted (lines) dark I-V-curves are shown in fig.5. The energy level of the recombination centre enters  $J_{rg}$  only via the term  $\cos[E_r - E_{r0}/kT]$  in eq.8. As  $\cosh(x)$  is an even function, only the absolute value  $|E_r - E_{r0}|$  can be extracted from a single I-V-curve. But because  $E_r - E_{r0}$  contains a temperature dependent and a temperature independent part, the energy level of the recombination centre can be deduced from the temperature dependence of the recombination parameters. In the case of the cell IS1, it is the level approx. 0.11eV above midband, and for IS2 approx. 0.07eV above midband.

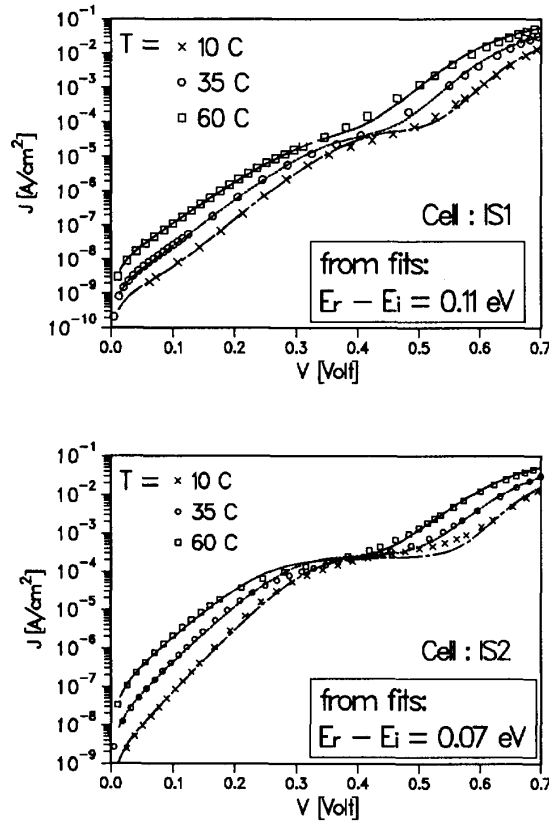


Fig.5: Dark I-V-curves of the cells IS1 and IS2 at different temperatures.  
Symbols: measured values  
Lines: eq.2 fitted to the curves [1]

For the cell IS2, the energy level of the recombination centre was corroborated by analysing the reverse I-V-characteristic by means of the I-V-T-method. This method allows one to identify recombination centres which dominate

the recombination current, yielding the so called activation energy  $E_A$ . From the value  $E_A = 0.673\text{eV}$  determined from the experimental data of IS2, the energy level  $E_r \approx E_i + 0.1\text{eV}$  was confirmed.

Two further examples of measured and fitted dark I-V-curves of high efficiency cells are shown in fig.6. They have the same type of recombination centre (= identical  $\tau_{n0}/\tau_{p0}$  and  $E_r - E_{r0}$  and same form of the curves), but  $\tau_{p0}$  of AL51.4 is 1.8 times smaller than of AL51.7, resulting in a 1.8 times higher recombination current (see eq.15).

For comparison, the best possible fit curves of the two-diode model are added in the graphs; the discrepancy can clearly be seen.

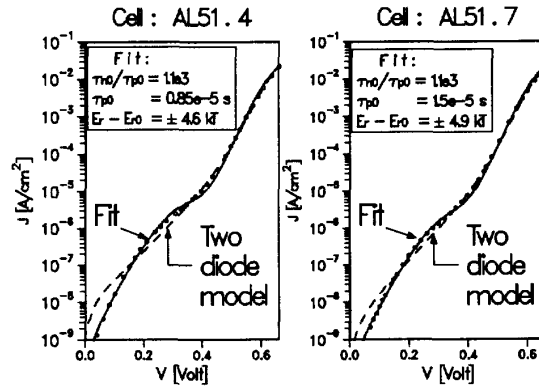


Fig.6: Dark I-V-curves of 2 ISE cells from the same batch.  
Symbols: measured values  
Dotted lines: best possible fit to the two-diode model  
Lines: eq.2 fitted to the curves [1]

#### DIODE QUALITY FACTOR $n_2$

Besides the striking deviations of the measured I-V-curves from the two-diode model in form of the "humps", we noticed that the value of the diode quality factor of the recombination current,  $n_2$ , often differs from the usually assumed value of  $n_2 = 2$ .

This can now be explained by superposition of several humps (and a shunt current). An example of this is shown in fig.7. The parameters used for this example are given in the figure caption.

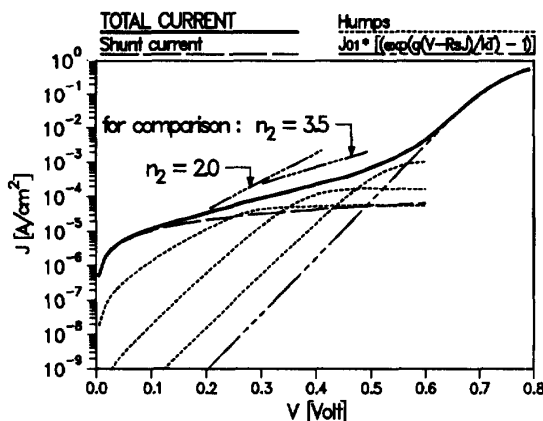


Fig.7: I-V-curve, resulting from the superposition of several current contributions with the following parameters:  
 - shunt current ( $R = 10^4 \Omega \text{cm}^2$ )  
 - hump 1:  $\tau_{n0} = 7 \cdot 10^{-10} \text{s}$ ,  $\tau_{p0} = 1 \cdot 10^{-6} \text{s}$ ,  $E_r - E_{r0} = \pm 10 \text{kT}$   
 - hump 2:  $\tau_{n0} = 1 \cdot 10^{-10} \text{s}$ ,  $\tau_{p0} = 4 \cdot 10^{-6} \text{s}$ ,  $E_r - E_{r0} = \pm 2 \text{kT}$   
 - hump 3:  $\tau_{n0} = 2 \cdot 10^{-11} \text{s}$ ,  $\tau_{p0} = 2 \cdot 10^{-7} \text{s}$ ,  $E_r - E_{r0} = \pm 15 \text{kT}$   
 - Shockley current  $J_{01} = 5 \cdot 10^{-13} \text{A/cm}^2$ ,  $R_s = 0.1 \Omega \text{cm}^2$   
 The slope of the recombination current corresponds to about  $n_2 \approx 3.5$

## DISCUSSION

Humps are seen especially in high efficiency cells, while commercial cells mainly show the deviation in the quality factor,  $n_2 \neq 2$ . This is plausible from the following reasons:

The high efficiency cells are built of very pure material, making the presence of a multitude of pollutants and thus recombination centres unprobable. Besides, at the energies found for the ISE cells of fig.5 and fig.6, silicon specific intrinsic energy levels caused by double interstitials and double vacancies are stated in [11]; according to [12], these levels are frequently found in silicon. The levels could be caused by the high phosphorus doping of the emitter and/or the thermal oxidation necessary for preparing the  $\text{SiO}_2$ -layer [8, 9, 10].

For cells which are not built under clean room conditions, a multitude of recombination centres can be expected. By superimposing the recombination currents related to the single recombination centres, a levelling of the single humps occurs, as seen in fig.7.

Depending on the distribution of energy levels, capture cross sections for electrons and holes and concentrations of the recombination centres, different slopes of the total I-V-curves and thus different values of  $n_2$  result.

## RESULTS AND SUMMARY

In this work we gave a quantitative analysis of the deviations of the form ("humps") as well as of the slope ( $n_2 \neq 2$ ) of dark I-V-curves of solar cells from the usual two-diode model.

The humps in the experimental I-V-curves were excellently fitted by the theoretical descriptions given here, allowing for recombination centres with recombination parameters  $E_r \neq E_i$  and  $\tau_{n0} \neq \tau_{p0}$  in the SRH-theory.

As for  $n_2 \neq 2$ , we showed how by superimposing several humps, a smooth I-V-curve with a slope deviating from  $n_2 = 2$  results.

## REFERENCES

- [1] J. Beier, Untersuchungen zur Anwendbarkeit des Superpositionsprinzips bei Silizium-Solarzellen, *doctoral thesis*, Freiburg, 1992 (in german)
- [2] C.T. Sah, R.N. Noyce, W. Shockley, Carrier Generation and Recombination in P-N Junctions and P-N Junction Characteristics, *Proc. of the IRE*, **45**(1957), pp.1228
- [3] S.C. Choo, Carrier Generation-Recombination in the Space-Charge Region of an Asymmetrical p-n Junction, *Solid-State Electronics*, **11**(1968), pp.1069
- [4] B.R. Chawla, H.K. Gummel, Transition Region Capacitance of Diffused p-n Junctions, *IEEE TED*, **18** No.3(1971), pp.178
- [5] J.J. Liou, F.A. Lindholm, Thickness of p/n junction space-charge layers, *J. Appl. Phys.*, **64** No.3(1988), pp.1249
- [6] S.M. Hu, P. Fahey, R.W. Dutton, On Models of Phosphorus Diffusion in Silicon, *J. Appl. Phys.*, **54** No.12(1983), pp.6912
- [7] M.A. Green, Intrinsic Concentration, Effective Densities of States, and Effective Mass in Silicon, *J. Appl. Phys.*, **67** No.6(1990), pp.2944
- [8] A. Armigliato, M. Servidori, S. Solmi, I. Vecchi, On the Growth of Stacking Faults and Dislocations Induced in Silicon by Phosphorus Predispotion, *J. Appl. Phys.*, **48** No.5(1977), pp.1806
- [9] H. Strunk, U. Gösele, B.O. Kolbesen, Interstitial Supersaturation near Phosphorus-Diffused Emitter Zones in Silicon, *Appl. Phys. Lett.*, **34** No.8(1979), pp.530
- [10] U.M. Gösele, T.Y.Tan, Equilibria, Nonequilibria, Diffusion, and Precipitation; in: *Materials Science and Technology vol 4: Electronic Structure and Properties of Semiconductors*, Hrsg. W. Schröter, Verlag VCH 1991
- [11] Hrsg. K.-H. Hellwege, O. Madelung, *Zahlenwerte und Funktionen aus Naturwissenschaft und Technik, III17a: Physik der Elemente der IV. Gruppe und der III-V Verbindungen*, Springer 1982
- [12] M. Schulz, Erlangen, *private communication*, 1992